Inorg. Chem. **2007**, *46*, 7458–7465

Unusual (μ-aqua)bis(μ-carboxylate) Bridge in Homometallic M(II) (M = Mn, Co and Ni) Two-Dimensional Compounds Based on the 1,2,3,4-Butanetetracarboxylic Acid: Synthesis, Structure, and Magnetic Properties

Laura Cañadillas-Delgado,[†] Oscar Fabelo,[†] Jorge Pasán,[†] Fernando S. Delgado,[†,‡] Francesc Lloret,[§] Miguel Julve,[§] and Catalina Ruiz-Pérez*,[†]

Laboratorio de Rayos X y Materiales Moleculares, Departamento de Física Fundamental II, Facultad de Física, Universidad de La Laguna, Av. Astrofísico Francisco Sánchez s/n, 38206 La Laguna (Tenerife), Spain, BM16—LLS European Synchrotron Radiation Facility, 6 Rue Jules Horowitz-BP 220 38043 Grenoble CEDEX 9, France, Instituto de Ciencia Molecular/ Departament de Química Inorgànica, Universitat de València, Poligono La Coma s/n, 46980 Paterna (València), Spain

Received April 9, 2007

The first coordination compounds of 1,2,3,4-butanetetracarboxylate anion (butca^{4-}) of the formula $[M_2(butca)(H_2O)_5]_n \cdot 2nH_2O$ [M = Mn(II) (**1**), Co(II) (**2**), and Ni(II) (**3**)] were prepared and their X-ray crystal structures and magnetic properties investigated. The three complexes have a very similar two-dimensional structure which consists of (4,4) networks, **1** and **2** being isostructural. The tetracarboxylate ligand acts as a 4-fold connector leading to two-dimensional (4,4) networks of metal atoms, this topology being possible because of its planar conformation. The nodes of these networks are formed by dinuclear motifs which exhibit the unusual (μ-aqua)bis(μ-carboxylate) bridging unit which is analogous to that observed in some molecules of biological interest. The variable-temperature magnetic susceptibility measurements of **1**–**3** show that **1** and **2** are antiferromagnetically coupled systems whereas **3** exhibits a ferromagnetic behavior. The analysis of the magnetic data of **1**–**3** through a simple dinuclear model allowed the determination of the values of the magnetic coupling (J) –3.6 (**1**), –1.2 (**2**), and +1.47 cm^{-1} (**3**) with the Hamiltonian being defined as $H = -JS_A \cdot S_B$. The countercomplementarity between the two bridges (aqua and syn–syn carboxylate) accounts for the trend exhibited by the values of the magnetic coupling in this family.

Introduction

Polynuclear metal complexes are currently of great interest, owing to their relevance to many important naturally occurring processes. The cooperative action of closely coupled dinuclear or multinuclear centers is required for several manganese enzymes to carry out their biological functions, for example, in arginase, Mn catalase, bacterial ribonucleotide reductase, or photosynthetic water oxidase.[1] Over the past decade, the field of coordination polymers has undergone an explosive growth.[2] In order for such coordination polymers to be potentially useful, it is essential that their structures can be rationally and predictably tuned via variation and functionalization of their constituent building blocks. Although the use of rigid ligands represents the most promising approach,[2] the incorporation of flexible groups as substituents can afford novel interesting networks.

Along this line and in the framework of our efforts to synthesize high-dimensional magnetic materials with divalent transition metal ions and polycarboxylate ligands,[3–6] we have

* To whom correspondence should be addressed. E-mail: caruiz@ull.es.
[†] Universidad de La Laguna.
[‡] BM16—LLS European Synchrotron Radiation Facility.
[§] Universitat de València.

(1) (a). Hola, R. H.; Kennepohl, P.; Solomon, E. I. *Chem. Rev.* **1996**, *96*, 2239. (b) Sträter, N.; Lipscomb, W. N.; Klabunde, T.; Krebs, B. *Angew. Chem., Int. Ed. Engl.* **1996**, *35*, 2024. (c) Dismukes, G. C. *Chem. Rev.* **1996**, *96*, 2990. (d) Kanyo, C. F.; Scolnick, L. R.; Ash, D. E.; Christianson, D. W. *Nature* **1996**, *383*, 554. (e) Khangulov, S. V.; Pessiki, P. J.; Barynin, V. V.; Ash, D. E.; Dismukes, G. C. *Biochemistry* **1995**, *34*, 2015. (f) Davies, J. F.; Hostomska, Z.; Hostomsky, Z.; Jordan, S. R.; Matthews, D. A. *Science* **1991**, *252*, 88. (g) Khangulov, S. V.; Barynin, V. V.; Voevodskaya, N. V.; Grebenko, A. I. *Biochim. Biophys. Acta* **1990**, *1020*, 305. (h) Willing, A.; Follmann, H.; Auling, G. *Eur. J. Biochem.* **1988**, *170*, 603. (i) Debus, R. J. *Biochim. Biophys. Acta* **1992**, *1102*, 269.
(2) (a) Zaworotko, M. J. *Chem. Soc. Rev.* **1994**, 283. (b) Batten, S. R.; Robson, R. *Angew. Chem., Int. Ed.* **1998**, *37*, 1461. (c) Janiak, C. *Angew. Chem., Int. Ed. Emgl.* **1997**, *36*, 1431. (d) Noro, S.; Kitaura, R.; Kondo, M.; Kitagawa, S.; Ishii, T.; Matsuzaka, H.; Yamashita, M. *J. Am. Chem. Soc.* **2002**, *124*, 2568.

10.1021/ic7006765 CCC: $37.00
Published on Web 08/11/2007

explored the coordination chemistry of the 1,2,3,4-butanetetracarboxylate (butca^{4-}) ligand whose structure was determined as the tetraammonium salt.[7] This tetracarboxylate ligand can act at the same time as a connector and as a 4-fold node through its four carboxylate groups toward the metal ions. Diamondoid or square grid networks can be envisaged for the butca-containing metal complexes depending on the conformation of the butca ligand. The (4,4) network will be favored if the planar conformation of the four carboxylate groups observed in its ammonium salt[4] is kept. Our first attempts on the complex formation between first row transition metal ions and butca^{4-} afforded three two-dimensional compounds of cobalt(II), manganese(II), and nickel(II) exhibiting the unusual (μ-aqua)bis(μ-carboxylate) bridging unit. The structure of the $M_2(\mu\text{-}H_2O)(\mu\text{-}O_2CR)_2$ core is analogous to that observed in hemerythrin[8] and various dinuclear complexes,[9−13] and it has been observed as a substructure in a few high-dimensional complexes.[14]

We present herein the synthesis, crystallographic analysis, and magnetic properties of the first butca-containing metal complexes of the formula $[M_2(butca)(H_2O)_5]_n \cdot 2nH_2O$ [M = Mn(II) (**1**), Co(II) (**2**), and Ni(II) (**3**)].

Experimental Section

Materials. Reagents and solvents used in all the syntheses were purchased from commercial sources and used without further purification. Elemental analyses (C, H) were performed on an EA 1108 CHNS−O microanalytical analyzer.

Preparation of the Complexes. $[M_2(butca)(H_2O)_5]_n \cdot 2nH_2O$ [M = Mn(II) (1), Co(II) (2) and Ni(II) (3)]. An aqueous solution of 1,2,3,4-butanetetracarboxylic acid 0.1 M (10 cm^3) was poured into a 0.1 M (20 cm^3) aqueous solution of the acetate salts of manganese(II) (**1**), cobalt(II) (**2**), or nickel(II) (**3**). The resulting mixture was sealed in a 45 cm^3 stainless-steel reactor with a Teflon liner and heated at 150 °C for 48 h.[15] After cooling, white (**1**), pink (**2**), and green (**3**) cubic crystals were collected from the Teflon liner and air-dried. This crystalline material was suitable for X-ray analyses, and therefore, it was used in all the measurements. Yield ca. 0.30 (**1**), 0.32 (**2**), and 0.38 g (**3**). Anal. Calcd for **1**: C, 20.61; H, 4.32. Found: C, 20.68. H, 4.41%. Anal. Calcd for **2**: C, 20.27; H, 4.25. Found: C, 20.33. H, 4.35%. Anal. Calcd for **3**: C, 20.20; H, 4.66. Found: C, 20.51. H, 4.57%.

Physical Techniques. Magnetic susceptibility measurements on polycrystalline samples of **1**−**3** were performed in a Quantum Design SQUID magnetometer in the temperature range 1.9−300 K operating at 0.1 T ($50 < T \leq 300$ K) and 250 G ($T \leq 50$ K). Diamagnetic corrections of the constituent atoms were estimated from Pascal's constants[16] being −211 (**1**) and -207×10^{-6} cm^3 mol^{-1} (**2** and **3**). The values of the experimental magnetic susceptibility were also corrected for the temperature-independent paramagnetism and the magnetization of the sample holder.

(3) (a) Ruiz-Pérez, C.; Hernández-Molina, M.; Lorenzo-Luis, P.; Lloret, F.; Cano, J.; Julve, M. *Inorg. Chem.* **2000**, *39*, 3845. (b) Hernández-Molina, M.; Lorenzo-Luis, P.; Ruiz-Pérez, C.; Lloret, F.; Julve, M. *Inorg. Chim. Acta* **2001**, *313*, 87. (c) Rodríguez-Martín, Y.; Ruiz-Pérez, C.; Sanchiz, J.; Lloret, F.; Julve, M. *Inorg. Chim. Acta* **2001**, *318*, 159. (d) Rodríguez-Martín, Y.; Sanchiz, J.; Ruiz-Pérez, C.; Lloret, F.; Julve, M. *Inorg. Chim. Acta* **2001**, *326*, 20. (e) Sanchiz, J.; Rodríguez-Martín, Y. Ruiz-Pérez, C.; Mederos, A.; Lloret, F.; Julve, M. *New J. Chem.* **2002**, *26*, 1624. (f) Rodríguez-Martín, Y.; Hernández-Molina, M.; Delgado, F. S.; Pasán, J.; Ruiz-Pérez, C. Sanchiz, J.; Lloret, F.; Julve, M. *CrystEngComm* **2002**, *4*, 440. (g) Rodríguez-Martín, Y.; Hernández-Molina, M.; Delgado, F. S.; Pasán, J.; Ruiz-Pérez, C.; Sanchiz, J.; Lloret, F.; Julve, M. *CrystEngComm* **2002**, *4*, 522. (h) Rodríguez-Martín, Y.; Hernández-Molina, M.; Sanchiz, J.; Ruiz-Pérez, C.; Lloret, F.; Julve, M. *Dalton* **2003**, 2359. (i) Hernández-Molina, M.; Lorenzo-Luis, P.; Gili, P.; Ruiz-Pérez, C. *Cryst. Growth Des.* **2003**, *3*, 273. (j) Delgado, F. S.; Sanchiz, J.; Ruiz-Pérez, C.; Lloret, F.; Julve, M. *CrystEngComm* **2003**, *5*, 280. (k) Delgado, F. S.; Sanchiz, J.; Ruiz-Pérez, C.; Lloret, F.; Julve, M. *Inorg. Chem.* **2003**, *42*, 5938. (l) Delgado, F. S.; Hernández-Molina, M.; Sanchiz, J.; Ruiz-Pérez, C.; Rodríguez-Martín, Y.; López, T.; Lloret, F.; Julve, M. *CrystEngComm* **2004**, *6*, 106.

(4) (a) Ruiz-Pérez, C.; Rodríguez-Martín, Y.; Hernández-Molina, M.; Delgado, F. S.; Pasán, J.; Sanchiz, J.; Lloret, F.; Julve, M. *Polyhedron* **2003**, *22*, 2111. (b) Pasán, J.; Delgado, F. S.; Rodríguez-Martín, Y.; Hernández-Molina, M.; Ruiz-Pérez, C.; Sanchiz, J.; Lloret, F.; Julve, M. *Polyhedron* **2003**, *22*, 2143.

(5) (a) Pasán, J.; Sanchiz, J.; Ruiz-Pérez, C.; Lloret, F.; Julve, M. *New J. Chem.* **2003**, *27*, 1557. (b) Pasán, J.; Sanchiz, J.; Ruiz-Pérez, C.; Lloret, F.; Julve, M. *Eur. J. Inorg. Chem.* **2004**, 4081. (c) Pasán, J.; Sanchiz, J.; Ruiz-Pérez, C.; Lloret, F.; Julve, M. *Inorg. Chem.* **2005**, *44*, 7794. (d) Pasán, J.; Sanchiz, J.; Ruiz-Pérez, C.; Campo, J.; Lloret, F.; Julve, M. *Chem. Commun.* **2006**, 2857.

(6) (a) Ruiz-Pérez, C.; Lorenzo-Luis, P.; Hernández-Molina, M.; Laz, M. M.; Delgado, F. S.; Gili, P.; Julve, M. *Eur. J. Inorg. Chem.* **2004**, 3873. (b) Fabelo, O.; Pasán, J.; Lloret, F.; Julve, M.; Ruiz-Pérez, C. *CrysEngComm* **2007**, in press.

(7) Pierrot, M.; Giorgi, M.; El Messaoudi, M.; Hasnaoui, A.; El Aatmani, M.; Lavergne, J. P. *Acta Crystallogr., Sect. C* **1996**, *52*, 731.

(8) Klotz, I. M.; Kurtz, D. M., Jr. *Acc. Chem. Res.* **1984**, *17*, 16.

(9) Coucouvanis, D.; Reynolds, R. A., III; Dunham, W. R. *J. Am. Chem. Soc.* **1995**, *117*, 7570.

(10) (a) Turpeinen, U.; Ahlgren, M.; Hamalainen, R. *Acta Crystallogr., Sect. B* **1982**, *38*, 1580. (b) Ahlgren, M.; Hamalainen, R.; Turpeinen, U. *Finn. Chem. Lett.* **1983**, 125. (c) Turpeinen, U.; Hamalainen, R.; Reedjik, J. *Polyhedron* **1987**, *6*, 1603. (d) Brown, D. A.; Glass, W. K.; Fitzpatrick, N. J.; Kemp, T. J.; Errington, W.; Clarkson, G. J.; Haase, W.; Kasrsten, F.; Mahdy, A. H. *Inorg. Chim. Acta* **2004**, *357*, 1411. (e) Burley, J. C.; Prior, T. J. *Acta Crystallogr., Sect. E* **2005**, *61*, m1422. (f) Hagen, K. S.; Lachicotte, R.; Kitaygorodskiy, A.; Elbouadili, A. *Angew. Chem., Int. Ed. Engl.* **1993**, *32*, 1321. (g) Corkery, R. W.; Hockless, D. C. R. *Acta Crystallogr., Sect. C* **1997**, *53*, 840. (h) Aromi, G.; Batsanov, A. S.; Christian, P.; Helliwell, M.; Parkin, A.; Parsons, S.; Smith, A. A.; Timco, G. A.; Winpenny, R. E. P. *Chem.-Eur. J.* **2003**, *9*, 5142. (i) Miao, Q.; Hu, M.-L.; Chen, F. *Acta Crystallogr., Sect. E* **2004**, *60*, m1314. (j) Hagen, K. S.; Lachicotte, R.; Kitaygorodskiy, A. *J. Am. Chem. Soc.* **1993**, *115*, 12617. (k) Kong, L.-L.; Huo, L.-H.; Gao, S.; Zhao, J.-G. *Acta Crystallogr., Sect. E* **2005**, *61*, m2485.

(11) Caneschi, A.; Ferraro, F.; Gatteschi, D.; Melandri, M. C.; Rey, P.; Sessoli, R. *Angew. Chem., Int. Ed.* **1989**, *28*, 1365.

(12) (a) Yu, S.-B.; Lippard, S. J.; Shweky, I. *A. Bino, Inorg. Chem.* **1992**, *31*, 3502. (b) Ye, B.-H.; Mak, T.; Williams, I. D.; Li, X.-Y. *Chem. Commun.* **1997**, 1813.

(13) (a) Turpeinen, U.; Ahlgren, M.; Hamalainen, R. *Finn. Chem. Lett.* **1977**, 246. (b) Turpeinen, U. *Finn. Chem. Lett.* **1976**, 173. (c) Ahlgren, M.; Hamalainen, R.; Turpeinen, U. *Cryst. Struct. Commun.* **1977**, *6*, 829. (d) Ahlgren, M.; Turpeinen, U. *Acta Crystallogr., Sect. B* **1982**, *38*, 276. (e) Ahlgren, M.; Turpeinen, U.; Hamalainen, R. *Acta Chem. Scand. A* **1978**, *32*, 189. (f) Turpeinen, U. *Finn. Chem. Lett.* **1977**, 36. (g) Kennard, C. H. L.; O'Reilly, E. J.; Smith, G. *Polyhedron* **1984**, *3*, 689. (h) Turpeinen, U. *Finn. Chem. Lett.* **1977**, 123. (i) Ye, B.-H.; Williams, I. D.; Li, X.-Y.; *J. Inorg. Biochem.* **2002**, *92*, 128. (j) Chaboussant, G.; Basler, R.; Gudel, H.-U.; Ochsenbein, S. T.; Parkin, A.; Parsons, S.; Rajaraman, G.; Sieber, A.; Smith, A. A.; Timco, G. A.; Winpenny, R. E. P. *Dalton Trans.* **2004**, 2758. (k) Eremenko, I. L.; Nefedov, S. E.; Sidorov, A. A.; Golubnichaya, M. A.; Danilov, P. V.; Ikorskii, V. N.; Schvedenkov, Y. G.; Novotortsev, V. M.; Moiseev, I. I. *Inorg. Chem.* **1999**, *38*, 3764.

(14) (a) Calvo-Pérez, V.; Ostrovsky, S.; Vega, A.; Pelikan, J.; Spodine, E.; Haase, W. *Inorg. Chem.* **2006**, *45*, 644. (b) Ayyappan, P.; Evans, O. R.; Lin, W. *Inorg. Chem.* **2001**, *40*, 4627. (c) Paluchowska, B.; Maurin, J. K.; Laciejewicz, J. *J. Coord. Chem.* **2000**, *51*, 335. (d) Uekusa, H.; Ohba, S.; Tokii, T. *Acta Crystallogr., Sect. C* **1995**, *51*, 625. (e) Lee, J.; Liu, Q.-D.; Motala, M.; Dane, J.; Gao, J.; Kang, Y.; Wang, S. *Chem. Mater.* **2004**, *16*, 1869. (f) Wu, C.-D.; Lu, C.-Z.; Zhuang, H.-H.; Juang, J.-S. *Z. Anorg. Allg. Chem.* **2003**, *629*, 693.

(15) Byrappa, K.; Yoshimura, M. *Handbook of Hydrothermal Technology: Technology for Crystal Growth and Materials Processing*; William Andrew Inc.: Salem, MA, 2001.

(16) Carlin, R. L. *Magnetochemistry*; Springer-Verlag: Berlin, Hendelberg, 1986.

Table 1. Crystal Data and Details of the Structure Determination of **1**−**3**

	1	**2**	**3**
T(K)	293(2)	293(2)	293(2)
formula	$C_8H_{20}Mn_2O_{15}$	$C_8H_{20}Co_2O_{15}$	$C_8H_{22}Ni_2O_{15}$
M_r	466.12	474.10	475.68
cryst syst	orthorhombic	orthorhombic	monoclinic
space group	*F2dd*	*F2dd*	*C2*/*c*
a, Å	8.1881(10)	8.0806(6)	27.743(10)
b, Å	28.3334(11)	28.0091(9)	8.066(11)
c, Å	28.5434(10)	28.1093(9)	16.146(13)
α, (°)	−	−	−
β, (°)	−	−	119.72(7)
γ, (°)	−	−	−
V, Å^3	6622.0(9)	6362.0(6)	3137.8(5)
Z	16	16	8
index ranges	$-10 < h < 9$	$-9 < h < 10$	$-26 < h < 36$
	$-36 < k < 34$	$-36 < k < 30$	$-10 < k < 9$
	$-36 < l < 33$	$-36 < l < 28$	$-20 < l < 15$
ρ_{calcd} (Mg m^{-3})	1.870	1.980	2.014
λ (Mo K$_\alpha$ Å)	0.71073	0.71073	0.71073
μ (Mo K$_\alpha$, mm^{-1})	1.602	2.166	2.482
Flack param	0.97(2)	0.025(11)	−
R1, $I > 2\sigma(I)$ (all)	0.0447 (0.0751)	0.0227 (0.0264)	0.0551 (0.0889)
wR2, $I > 2\sigma(I)$ (all)	0.0791 (0.0866)	0.0475 (0.0483)	0.0964 (0.1058)
measured reflns (R_{int})	12 928 (0.0667)	15 492 (0.0247)	13 821 (0.0498)
independent reflns ($I > 2\sigma(I)$)	3516 (2645)	3580 (3366)	3569 (2629)
cryst size (mm^3)	0.06 × 0.08 × 0.10	0.08 × 0.2 × 0.16	0.26 × 0.36 × 0.6

Crystallographic Data Collection and Structural Determination. The cubic single crystals of **1**−**3** were mounted on a Bruker-Nonius KappaCCD diffractometer, and the crystallographic data were collected at 293(2) K using graphite-monochromated Mo K$_\alpha$ radiation ($\lambda = 0.71073$ Å). The data collection was carried out with $\varphi-\omega$ scans in the θ range 4.0−27.5° (**1**), 4.6−27.5° (**2**), and 5.0−27.5° (**3**). A summary of the crystallographic data and structure refinement is given in Table 1. The crystal structures were solved by direct methods and refined with the full-matrix least-squares technique on F^2 using the *SHELXS-97* and *SHEXL-97* programs[17] included in the WINGX software package.[18] All non-hydrogen atoms were refined anisotropically. The water molecules O(2w) and O(3w) in all compounds have an occupation of 0.5, indicating that a water molecule is alternatively situated in each position within the crystal. The hydrogen atoms of the butca ligand were located from difference maps and refined with isotropic temperature factors. The hydrogen atoms of the water molecules were located from difference maps for compound **2**. The final geometrical calculations and the graphical manipulations were carried out with *PARST95*,[19] *PLATON*,[20] and *DIAMOND*[21] programs. Selected bond lengths and distances for **1**−**3** are listed in Table 2.

Description of the Structures

$[M_2(butca)(H_2O)_5]_n\cdot 2nH_2O$ [M = Mn(II) (1) and Co(II) (2)]. Complexes **1** and **2** are isostructural. Their crystal structure simultaneously consists of bis(μ-carboxylate)- and μ-aqua-bridged dimanganese(II) (**1**)/dicobalt(II) (**2**) units (see Figure 1a) which are linked through the fully deprotrotonated tetracarboxylate butca^{4-} ligand to form a (4,4) square grid that grows parallel to the *ac* plane (see Figure 2a). The two metal atoms of this dinuclear unit of **1** and **2** [M(1) and M(2)] are crystallographically independent. The butca group acts as an asymmetric 4-fold connector, a situation which is favored by the conformation of the carboxylate groups where the M(1) atom is a node. A (4,4) layered structure arises, and it is formed by squares and rectangles of dimensions ca. 5.0 × 5.0 and 7.0 × 4.5 Å^2, respectively, where the other metal atom [M(2)] of the dinuclear unit is located alternatively above and below of the small squares of the (4,4) network, with one M(2) per square. The sheets are stacked

Table 2. Selected Interatomic Bond Lengths (Å) and Angles (deg) in Compounds **1**−**3a**,**b**

Bond Lengths

1		**2**		**3**	
Mn(1)−O(8a^1)	2.151(3)	Co(1)−O(8a^1)	2.0686(17)	Ni(1)−O(2)	2.032(3)
Mn(1)−O(6)	2.164(4)	Co(1)−O(6)	2.0777(17)	Ni(1)-O(4b^2)	2.039(3)
Mn(1)−O(3c^1)	2.170(4)	Co(1)−O(3c^1)	2.0966(17)	Ni(1)−O(5)	2.080(3)
Mn(1)−O(1b^1)	2.190(3)	Co(1)−O(1b^1)	2.1069(17)	Ni(1)−O(8a^2)	2.084(3)
Mn(1)−O(8W)	2.207(3)	Co(1)−O(8W)	2.125(2)	Ni(1)−O(8W)	2.108(4)
Mn(1)−O(7W)	2.247(3)	Co(1)−O(7W)	2.1314(17)	Ni(1)−O(7W)	2.066(3)
Mn(2)−O(7a^1)	2.150(4)	Co(2)−O(7a^1)	2.0532(18)	Ni(2)−O(3b^2)	2.005(3)
Mn(2)−O(5)	2.131(4)	Co(2)−O(5)	2.0704(18)	Ni(2)−O(1)	2.013(3)
Mn(2)−O(4W)	2.177(3)	Co(2)−O(4W)	2.069(2)	Ni(2)−O(4W)	2.071(4)
Mn(2)−O(6W)	2.260(4)	Co(2)−O(6W)	2.169(2)	Ni(2)−O(6W)	2.066(4)
Mn(2)−O(7W)	2.196(3)	Co(2)−O(7W)	2.0764(16)	Ni(2)−O(7W)	2.038(3)
Mn(2)−O(5W)	2.200(4)	Co(2)−O(5W)	2.0775(19)	Ni(2)−O(5W)	2.125(4)

μ-Oxo Bridge Data

1		**2**		**3**	
Co(1)···Co(2)	3.5107(4)	Mn(1)···Mn(2)	3.6140(8)	Ni(1)···Ni(2)	3.4474(11)
Co(1)−O7W−Co(2)	113.10(8)	Mn(1)−O7W−Mn(2)	108.85(13)	Ni(1)−O7W−Ni(2)	114.28(15)

μ-Oxo Bridge Hydrogen Bond Data

	D−H	D···A	D−H···A
		1	
O(7w)−H···O(2b^1)	0.86(3)	2.545(3)	162(3)
O(7w)−H···O(4c^1)	0.88(2)	2.578(3)	165(2)
		2	
O(7w)−H···O(2b^1)		2.570(5)	
O(7w)−H···O(4c^1)		2.579(5)	
		3	
O(7w)···O(6)		2.542(5)	
O(7w)···O(7a^2)		2.522(6)	

[a] Symmetry codes: a^1 = $x-1, y, z$; b^1 = $x-1/4, -y+7/4, z+1/4$; c^1 = $x-5/4, -y+7/4, z+1/4$; a^2 = $-x, -y, -z$; b^2 = $-x+1/2, -y+1/2, -z$. [b] A= acceptor and D = donor.

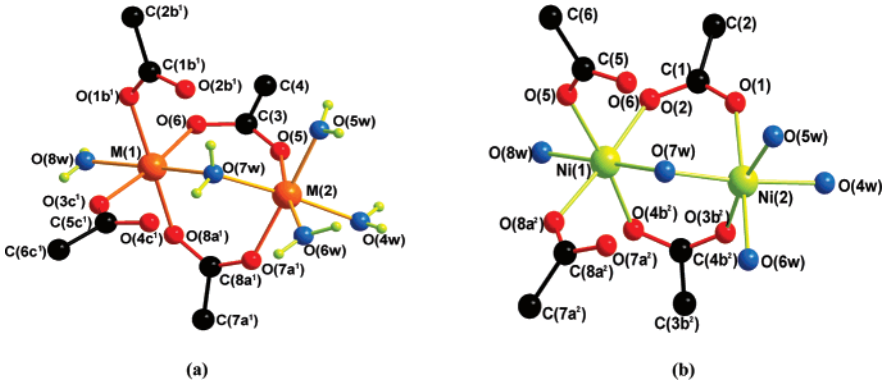

Figure 1. Perspective views of the dinuclear core in (a) **1** and **2** and (b) **3**. M = Co(II) (**1**) and Mn(II) (**2**). Symmetry codes: $a^1 = x - 1, y, z$; $b^1 = x - 1/4, -y + 7/4, z + 1/4$; $c^1 = x - 5/4, -y + 7/4, z + 1/4$; $a^2 = -x, -y, -z$; $b^2 = -x + 1/2, -y + 1/2, -z$.

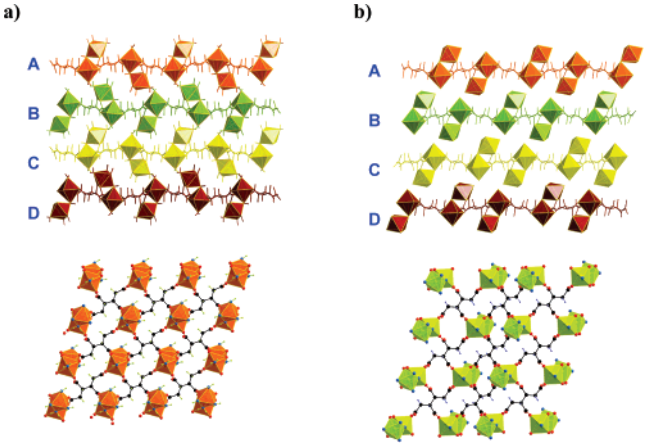

Figure 2. Views of the layers in **1**−**3** focusing (top) on the packing of adjacent planes for **1** and **2** (a) and **3** (b) along the *b* (**1** and **2**) and *c* (**3**) axes; (bottom) on a single layer for **1** and **2** (a) and **3** (b) down the *b* (**1** and **2**) and *c* (**3**) axes.

along the *b* direction exhibiting the ABCDABCDABCD sequence [see Figure 2a (top)]. The A, B and C, D pairs are related by a rotation of 180° in the *c* axis, respectively, whereas the pair of layers A and C are related by a translation of *a*/2 along the *a* direction. Weak hydrogen bonds involving the crystallization and coordinated water molecules and free carboxylate oxygen atoms link the layers to build up a supramolecular three-dimensional network.

The two metal centers of the dinuclear nodes are bridged by two carboxylate groups in the syn−syn coordination mode plus an oxygen atom from a water molecule. The values of the M(1)···M(2) separation are 3.6140(8) (**1**) and 3.5107(4) Å (**2**) and those of the M(1)−O(7w)−M(2) angle are 108.85(13)° (**1**) and 113.10(8)° (**2**) (Table 2). The shortening of the M(1)···M(2) separation in **2** with respect to that in **1** in spite of the larger angle at the aqua bridge in the former is due to the shorter values of the metal-to-aqua bonds in **2** (Table 2). Hydrogen-bond interactions [O···O distances ranging from 2.522(6) to 2.579(5) Å] between the bridging water molecule and the uncoordinated carboxylate-oxygen atoms of the carboxylate ligands at M(1) contribute to the stabilization of the dinuclear entity (Table 2). The structural features concerning the dinuclear cores of **1** and **2** are in agreement with those reported for other cobalt(II)[7,8] and manganese(II)[9,10] complexes containing the (μ-aqua)bis(μ-carboxylate) unit.

M(1) and M(2) are six-coordinated in a somewhat distorted octahedral environment (see Figure 1a). Four oxygen atoms [O(1b^1), O(3c^1), O(6), and O(8a^1)] from four different carboxylate groups belonging to different butca ligands and two water molecules [O(7w) and O(8w)] build the coordination polyhedron around M(1). Two of these carboxylate groups [those containing the O(6) and O(8a^1) atoms] and a water molecule [O(7w)] act as bridges toward M(2). The remaining uncoordinated oxygen atoms from the other carboxylate groups [those containing the oxygen atoms O(1b^1) and O(3c^1)] establish strong hydrogen bonds with the bridging water molecule [O(7w)]. The six coordination around M(2) is achieved in a different manner from that of M(1). Two oxygen atoms [O(5) and O(7a^1)] from carboxylate groups of the butca ligand and four water molecules [O(4w), O(5w), O(6w), and O(7w)] build the octahedral environment around M(2). The bond distances between the metal ions and the coordinated water molecules are slightly longer [average values of 2.227(2) (**1**) and 2.128(2) Å (**2**)] than those related to the oxygen atoms of the carboxylate groups [mean values of 2.169(4) (**1**) and 2.088(2) Å (**2**)].

There is one crystallographically independent butca ligand in the crystal structure of **1** and **2**. Two of the four carboxylate groups [O(5)−C(3)−O(6) and O(7)−C(8)−O(8)] of the butca group adopt the bis-monodentate bridging mode in the syn−syn conformation toward M(1) and M(2) and M(1f^1) and M(2f^1) [$f^1 = x + 1, y, z$] respectively, whereas the other two [O(1)−C(1)−O(2) and O(3)−C(5)−O(4)] act as monodentate ligands toward M(1d^1) [$d^1 = x + 1/4, -y + 7/4, z - 1/4$] and M(1e^1) [$e^1 = x + 5/4, -y + 7/4, z - 1/4$] (see Figure 3a). The shortest intralayer separations between the M(1) atoms [M(1)···M(1d^1) in Figure 3a] are 7.594(2) (**1**) and 7.459(2) Å (**2**), values which correspond to the diagonal of the squares of the (4,4) network. These values are shorter than those corresponding

(17) Sheldrick, G. M. *SHELXL-97 and SHELXS-97*; Universität Göttingen: Göttingen, Germany, 1998.
(18) Farrugia, L. J. *J. Appl. Crystallogr.* **1999**, *32*, 837.
(19) Nardelli, M. *J. Appl. Crystallogr.* **1995**, *28*, 659.
(20) Speck, A. L. *Acta Crystallogr., Sect. A* **1990**, *34*, 46.
(21) *DIAMOND 2.1d, Crystal Impact GbR, CRYSTAL IMPACT*; K. Brandenburg and H. Putz GbR: Bonn, Germany, 2000.

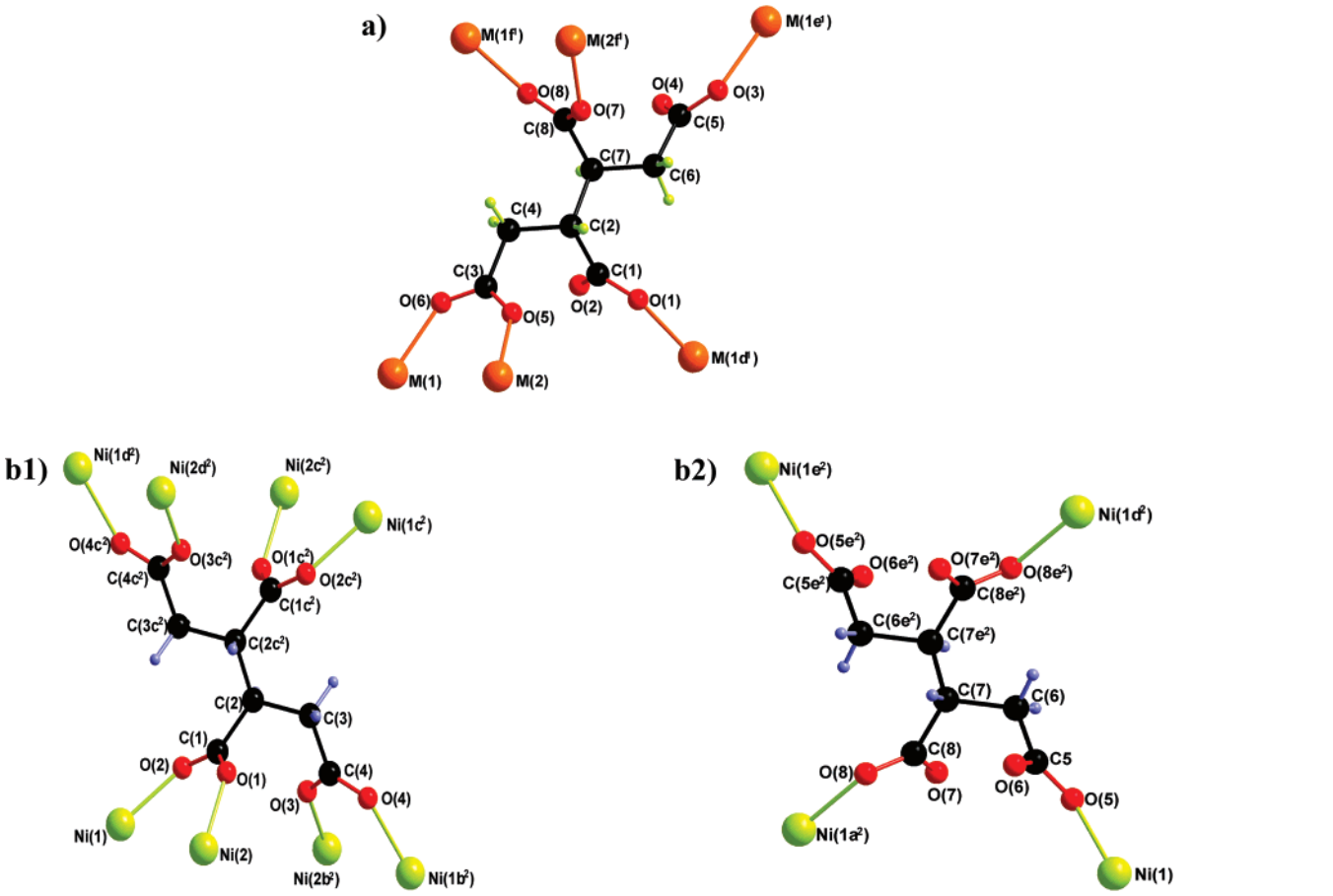

Figure 3. Coordination modes of the butca ligand in **1** and **2** (a) and **3** (b1 and b2) along with the numbering scheme. M = Co(II) in **1** and Mn(II) in **2.** Symmetry codes: $d^1 = x + 1/4, -y + 7/4, z - 1/4$; $e^1 = x + 5/4, -y + 7/4, z - 1/4$; $f^1 = x + 1, y, z$; $c^2 = -x + 1/2, -y - 1/2, -z$; $d^2 = x, y - 1, z$; $e^2 = -x, -y - 1, -z$.

to the diagonal of the rectangles of the (4,4) network [8.188(2) (**1**) and 8.081(2) Å (**2**) for M(1)···M(1e[1])].

$[Ni_2(butca)(H_2O)_5]_n \cdot 2nH_2O$ (3). The crystal structure of **3** is very similar to that of **1** and **2** described above. The (μ-aqua)bis(μ-carboxylate)dinickel(II) entitities present in **3** (see Figure 1b) are linked through butca ligands to form a (4,4) network with squares and rectangles (see Figure 2b) as in **1** and **2**. One of the nickel atoms [Ni(1)] of the dinuclear unit acts as a four-node as M(1) in **1** and **2**, but the difference being that two Ni(2) atoms in **3** are located (one above and the other below) over the same square, leaving empty squares in an alternative fashion. The sheets are stacked perpendicularly to the *ab* plane [see Figure 2b (top)], and they are linked through hydrogen bonds involving crystallization water molecules located in the interlayer space to build a three-dimensional supramolecular network.

The dinickel(II) unit of **3** exhibits the same structural pattern observed for the related ones in **1** and **2**. The Ni···Ni separation is 3.4474(11) Å, a value which is slightly shorter than those in **1** and **2**. However, the Ni(1)−O(7w)−Ni(2) angle is larger than those observed in **1** and **2**. This contradictory situation is due to a shortening of the nickel-to-water-oxygen at the bridge (see Table 2b). Anyway, these values in **3** are in agreement with those reported for other (μ-aqua)bis(μ-carboxylate)dinickel(II) units.[11] The main differences between the structures of the dinuclear units of **1**−**3** concern the torsion angles of the M(1)−O···O−M(2) carboxylate bridges and a subtle twist of M(2) along the O(4w)−Ni(2)−O(7w) vector.

There are two crystallographically independent butca ligands in **3**, L1 [C(1)−C(4)] and L2 [C(5)−C(8)] (Figure 3b). Both act as 4-fold connectors in the same way. The four carboxylate groups of L1 adopt the monodentate coordination mode (Figure 3b2) whereas those of L2 act as bis-monodentate bridges in the syn−syn conformation (Figure 3b1). It deserves to be noted that the coordination mode of each of the two butca ligands in **3** corresponds with each half of the crystallographically unique butca ligand in **1** and **2**. The shortest intralayer Ni···Ni separation through the butca ligands in **3** is 5.944(2) Å, a value which corresponds to the diagonal of the small squares of the (4,4) network and that is much shorter than the related ones in **1** and **2**.

Magnetic Properties of 1−3. The magnetic properties of **1** under the form of $\chi_M T$ versus T plot (χ_M is the magnetic susceptibility per two Mn(II) ions] are shown in Figure 4. $\chi_M T$ at room temperature is 8.20 $cm^3\ mol^{-1}$ K, a value which is close to that expected for two magnetically non-interacting single-ion sextuplet spin states ($\chi_M T$ = 8.75 $cm^3\ mol^{-1}$ K with g = 2.0). Upon cooling, $\chi_M T$ decreases smoothly in the high-temperature range and it exhibits a fast decrease at $T < 100$ K to reach a value of 0.2 $cm^3\ mol^{-1}$ K at 2.0 K. A maximum of the magnetic susceptibility occurs at 15 K (see

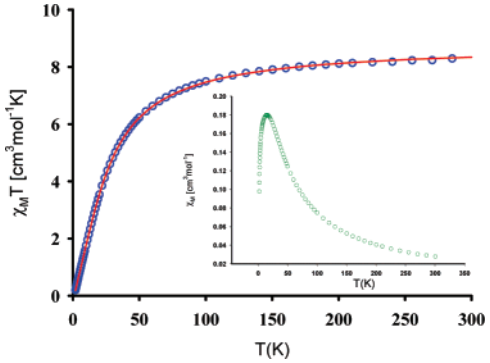

Figure 4. Temperature dependence of the $\chi_M T$ product for **1**: (○) experimental data; (− − −) best-fit curve (see text). The inset shows the χ_M vs T plot in the region of the maximum.

inset of Figure 4). This behavior is indicative of significant antiferromagnetic coupling between two $S = 5/2$ spin states leading to a low-lying spin singlet.

Although **1** is a two-dimensional compound, the presence of the(μ-aqua)bis(μ-carboxylate)dimanganese(II) cores with a Mn···Mn separation of 3.6140(8) Å which are well isolated from each other [the shortest interdimer metal−metal separation is greater than 5.9 Å, and it goes through the long Mn−O−C−C−C−O−Mn pathway)] allowed us to consider the magnetic behavior of this compound as due to the dinuclear entity (the same applies for **2** and **3**). Consequently, the magnetic data of **1** were analyzed in terms of an isotropic exchange interaction for a dinuclear species ($H = -JS_A \cdot S_B$ with $S_A = S_B = 5/2$) through the expression (eq 1)

$$\chi_M = \frac{2N\beta^2 g^2(x + 5x^3 + 14x^6 + 30x^{10} + 55x^{15})}{kT(1 + 3x + 5x^3 + 7x^6 + 9x^{10} + 11x^{15})} \qquad (1)$$

with $x = \exp(J/kT)$. The parameters N, β, g, and k have their usual meanings. Best-fit parameters are $J = -3.6$ cm^{-1}, $g = 2.0$ and $R = 3.0 \times 10^{-5}$ where R is the agreement factor which is defined as $\sum[(\chi_M T)_{obs} - (\chi_M T)_{calcd}]^2/\sum[(\chi_M T)_{obs}]$.[2] The calculated curve matches very well the magnetic data in the whole temperature range. The antiferromagnetic coupling found for **1** lies within the range observed for other dinuclear manganese(II) complexes having the same (μ-aqua)bis(μ-carboxylate) exchange pathway [$-J$ values ranging from 2.5 to 5.9 cm^{-1}; see Table 3].[11,12]

The magnetic properties of **2** under the form of $\chi_M T$ versus T plot (χ_M is the magnetic susceptibility per two Co(II) ions] are shown in Figure 5. At room temperature, $\chi_M T$ is equal to 5.90 cm^3 mol^{-1} K (μ_{eff} per Co^{II} of 4.86 μ_B). Upon cooling, $\chi_M T$ first decreases smoothly until $T \approx 30$ K, and at lower temperatures it exhibits an abrupt decrease to reach a value of 1.0 cm^3 mol^{-1} K at 1.9 K. No maximum is observed in the magnetic susceptibility in the temperature range explored. These data allow us to get two conclusions. First, the value of the μ_{eff} per cobalt atom at room temperature for **2** is larger than that expected for the spin-only case ($\mu_{eff} = 3.87\ \mu_B$ with $S_{Co} = 3/2$), indicating that the distortion of the octahedral symmetry of Co^{II} in **2** is not so large as to induce the total quenching of the $^4T_{1g}$ ground state. Second, having in mind that only the ground Kramers doublet of a high-spin cobalt(II) ion is populated at 1.9 K with an effective spin $S_{eff} = 1/2$ and a value of the Lande factor $g = 4.3$,[16,22] the calculated value of $\chi_M T$ for two magnetically isolated spin doublets with this g value is ca. 1.73 cm^3 mol^{-1} K. As this value is well above that observed for **2** at 1.9 K (ca. 1.0 cm^3 mol^{-1} K), there is no doubt about the occurrence of a significant antiferromagnetic coupling between the cobalt(II) ions in **2**.

Taking into account that **1** and **2** are isostructural and that in the case of **2** the sextet and quartet Kramers upper levels of the octahedral cobalt(II) ion cannot be neglected in calculating the susceptibilities at higher temperatures and not only because of their thermal population, since they also give rise to a large second-order Zeeman effect, the orbital reduction factor (x) and the spin−orbit coupling parameter (λ) together with the magnetic coupling (J) are the variable parameters to account for the magnetic properties of **2**. The Lines theory[23] of polynuclear compounds of cobalt(II) allows this treatment, the corresponding susceptibility expression for a dicobalt(II) unit being given by eq 2

$$\chi_M = \frac{2N\beta^2[g(T)]^2}{kT[3 + \exp(-25J/9kT)]} \qquad (2)$$

where $g(T)$ is a temperature-dependent g factor which needs to be evaluated for each T value in order to generate the theoretical χ_M vs T curve.[23,24] The best fit of the magnetic data gives $J = -1.2$ cm^{-1}, $\lambda = -133$ cm^{-1}, $x = 0.77$, and $R = 1.4 \times 10^{-5}$. The calculated curve matches the experimental data quite well, the small deviations being most likely due to the fact that the Lines theory was derived for six-coordinate Co(II) with O_h symmetry. The nature of the magnetic coupling in **2** is the same than that observed in the parent dinuclear cobalt(II) complex of formula Et$_4$N[Co$_2$(μ-H$_2$O)(μ-OAc)$_2$(OAc)$_3$(py)$_2$] (Et$_4$N = tetraethylammonium, OAc = acetate, and py = pyridine) where a J value of −0.4 cm^{-1} was calculated through the isotropic Hamiltonian $H = -JS_A \cdot S_B$,[6] the value of the intramolecular cobalt−cobalt separation [3.458(4) Å] and that of the angle at the aqua bridge [112.9(2)°] for this complex being very close to those of **2** [3.5107(4) Å and 113.10(8)°].

The magnetic properties of **3** under the form of $\chi_M T$ vs T plot [χ_M being the magnetic susceptibility per two Ni(II) ions] are shown in Figure 6. At room temperature, $\chi_M T$ is equal to 2.50 cm^3 mol^{-1} K, a value which is as expected for two magnetically isolated spin triplets ($\chi_M T = 2.42$ cm^3 mol^{-1} K with $g = 2.20$). Upon cooling, $\chi_M T$ continuously increases to reach a maximum of 2.97 cm^3 mol^{-1} K at 5.5 K, and then it decreases to 2.64 cm^3 mol^{-1} K at 1.9 K. This curve is typical of a ferromagnetically coupled nickel(II) dimer, the decrease at low temperatures being due to zero-field splitting effects and/or intermolecular interactions.

(22) (a) Herrera, J. M.; Bleuzen, A.; Dromzée, Y.; Julve, M.; Lloret, F.; Verdaguer, M. *Inorg. Chem.* **2003**, *42*, 7052. (b) Rodríguez, A.; Sakiyama, H.; Masciocchi, N.; Galli, S.; Gálvez, N.; Lloret, F.; Colacio, E. *Inorg. Chem.* **2005**, *44*, 8399. (c) Mishra, V.; Lloret, F.; Mukherjee, R. *Inorg. Chim. Acta* **2006**, *359*, 4053.
(23) Lines, M. E. *J. Chem. Phys.* **1971**, *55*, 2977.
(24) De Munno, G.; Julve, M.; Lloret, F.; Faus, J.; Caneschi, A. *J. Chem. Soc., Dalton Trans.* **1994**, 1175.

Table 3. Structural and Magnetic Details for Dinuclear (μ-aqua)bis(μ-carboxylate)-Bridged Manganese(II) Complexes

compound[a]	chromophore	Mn−O(w)−Mn/deg	Mn···Mn[b]/Å	J[c]/cm^{-1}	ref
$[Mn_2(\mu\text{-}H_2O)(\mu\text{-}OAc)_2(Im)_4(OAc)_2]$	MnN_2O_4	114.4(2)	3.777(1)	−2.52	9b
$[Mn_2(F_5C_2COO)_4(H_2O)3L^I{}_2]$	MnO_6	114.6(3)	3.739(2)	−3.3	8
$[Mn_2(H_2O)(piv)_4(Me2bpy)_2]$	MnN_2O_4	110.2(1)	3.5950(9)	−5.46	9a
$[Mn_2(H_2O)(OAc)_4(tmeda)_2]$	MnN_2O_4	110.0(2)	3.621(2)	−5.90	9a
1	MnO_6	108.8(1)	3.6140(8)	−3.6	this work

[a] Abbreviations: OAc = acetate, Im = Imidazole, L^I = 2-ethyl-4,4,5,5-tetramethyl-3-oxo-4,5-dihydro-1*H*-imidazolyl-1-oxyl, piv = pivalate, Me_2bpy = 4,4′-dimethyl-2,2′-bipyridine, tmeda = *N*,*N*,*N*′,*N*′-tetramethylethylenediamine. [b] Intramolecular separation. [c] Magnetic exchange coupling parameter based on the Hamiltonian $H = -JS_1 \cdot S_2$.

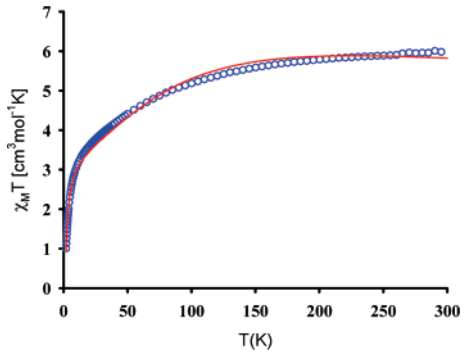

Figure 5. Temperature dependence of the $\chi_M T$ product for **2**: (○) experimental data; (− − −) best-fit curve (see text).

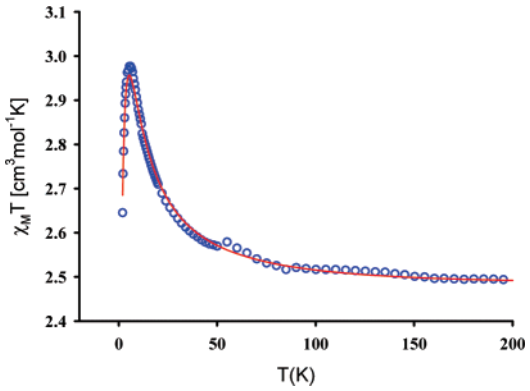

Figure 6. Temperature dependence of the $\chi_M T$ product for **3**: (○) experimental data; (− − −) best-fit curve (see text).

Assuming that the magnetic properties of **3** are due to the (μ-aqua)bis(μ-carboxylate)dinickel(II) core and the fact that the ground state for a nickel(II) ion in an octahedral environment is orbitally nondegenerate, it is possible to represent the intradimer magnetic interaction, J, with the isotropic spin Hamiltonian $H = -JS_A \cdot S_B$. Although nickel(II) in axial symmetry can have a large zero-field splitting (D), the magnetic behavior of a nickel(II) dimer can be analyzed through this isotropic Heisenberg Hamiltonian when a relatively strong antiferromagnetic coupling is involved. In the case of a weak antiferromagnetic interaction or when the coupling is ferromagnetic (as occurs in **3**), the effect of D can be relevant to describe the magnetic behavior at low temperatures. Following previous works where the effect of D on the magnetic susceptibility of nickel(II) dimers was considered,[25,26] we have analyzed the magnetic susceptibility data of **1** by the corresponding expression derived through the Hamiltonian $H = -JS_A \cdot S_B - D(S_{zA}{}^2 + S_{zB}{}^2)$. The best-fit values are $J = +1.47$ cm^{-1}, $D = 7.2$ cm^{-1}, and $g = 2.21$ with $R = 1.5 \times 10^{-5}$. The computed curve nicely follows the experimental data in the whole temperature range investigated. Although there some examples of reported structures of dinuclear nickel(II) complexes having the (μ-aqua)bis(μ-carboxylate)dinickel(II) core,[13] the magnetic properties of only one of them, $[Ni_2(\mu\text{-}H_2O)(\mu\text{-}OOCCMe_3)_2(OOCCMe_3)_2(HOOCCMe_3)_4]$ ($HOOCCMe_3$ = pivalic acid), were investigated, the magnetic coupling being ferromagnetic ($J = +5.2$ cm^{-1}).[13i] The shorter intramolecular nickel−nickel separation in this last compound [3.361(1) vs 3.447(4) Å in **3**] which is related to the smaller value of the angle at the aqua bridge [111.24(11)° vs 114.18(15)° in **3**] is most likely responsible for the somewhat stronger magnetic coupling in the pivalate-containing compound.

In order to understand the trend exhibited by the values of the magnetic coupling in **1**−**3** and in particular the ferromagnetic coupling observed for **3**, one has to focus on the simultaneous presence of two exchange pathways, the syn−syn carboxylate and the aqua molecule. For the first bridging ligand, it is well-known that the syn−syn conformation causes antiferromagnetic coupling, as evidenced by the large number of magneto-structural studies on acetato-bridged dicopper(II) complexes.[27] As far as the second bridge is concerned, although no data are available, ferromagnetic interactions are observed for di- and trinuclear nickel(II) complexes through the monoatomic oxo(phenolate) bridge with values of the Ni−O−Ni angle smaller than 93.5° (magic angle), the magnetic interaction being antiferromagnetic for larger values of this angle.[28] Looking at the value of the angle at the aqua bridge in **3** [114.28(15)° for N(1)−O(7w)−Ni(2)], an antiferromagnetic coupling would be expected through Ni−μ-H_2O−Ni. However, when the bridging ligands are different, the two bridges may add or counterbalance their effects. This problem was treated by Nishida et al.[29] and McKee et al.,[30] these phenomena being known as orbital complementarity and countercomplementarity, respectively. It is now clear that the syn−syn carboxylate with either the end-on azido,[31] oxo(alkoxo),[32] or hydroxo[33] as bridges exhibit

(25) (a) Ginsberg, A. P.; Martin, R. L.; Brookes, R. W.; Sherwood, R. C. *Inorg. Chem.* **1972**, *11*, 2884. (b) Journaux, Y. *Thèse de troisième cycle*; Orsay, 1978.
(26) De Munno, G.; Julve, M.; Lloret, F.; Derory, A. *J. Chem. Soc., Dalton Trans.* **1993**, 1179.
(27) Rodríguez, -Fortea, A.; Alemany, P.; Alvarez, S.; Ruiz, E. *Chem.-Eur. J.* **2001**, *7*, 627.
(28) Bu, X. H.; Du, M.; Zhang, L.; Liao, D. Z.; Tang, J. K.; Zhang, R. H.; Shionoya, M. *J. Chem. Soc., Dalton Trans.* **2001**, 593.
(29) Nishida, Y.; Kida, S. *J. Chem. Soc., Dalton Trans.* **1986**, 2633.
(30) McKee, V.; Zvagulis, M.; Reed, C. A. *Inorg. Chem.* **1985**, *24*, 2914.
(31) Thompson, L. K.; Tandom, S. S.; Lloret, F.; Cano, J.; Julve, M. *Inorg. Chem.* **1997**, *36*, 3301.
(32) Tudor, V.; Kravtsov, V. Ch.; Julve, M.; Lloret, F.; Simonov, Y. A.; Averkiev, B. B.; Andruh, M. *Inorg. Chim. Acta* **2005**, *358*, 2066.

orbital countercomplementarity, the magnetic coupling between the copper(II) ions through these pair of bridges being ferromagnetic. Consequently, the ferromagnetic coupling observed in **3** is most likely due to countercomplementary effects. However, when the number of magnetic orbitals on each spin carrier is increased [from two in nickel(II) to three in Co(II) and five in Mn(II) in the present family] the possibilities of net overlap between the magnetic orbitals increase and the antiferromagnetic terms associated to them counterbalance the countercomplementary effects, the magnetic interaction becoming antiferromagnetic as observed for **1** and **2**.

Conclusions

The first three new coordination compounds based on butca have been synthesized and magneto-structurally characterized. They exhibit two-dimensional arrangements where both the divalent metal ions and the tetradentate ligand act as 4-fold nodes. The metal ions are grouped in dinuclear entities within the 2D network showing the unusual (μ-aqua)-bis(μ-carboxylate) bridge. The investigation of whether rodlike ligands such as 4,4′-bipyridine or pyrazine could connect the layers to build a three-dimensional structure where the interlayer space may be tuned is in progress. The magnetic properties of **1**−**3** range from the antiferromagnetic interactions exhibited by the manganese(II) complex to the ferromagnetic interactions of the nickel(II) compound. These behaviors are explained on the basis of countercomplementarity and the synthesis of the related copper(II) complex where a ferromagnetic interaction is expected is in progress.

Acknowledgment. Financial support from Spanish Ministerio de Educación y Ciencia through projects MAT2004-03112, CTQ2004-03633 and "Factoría de Cristalización" (Consolider-Ingenio2010, CSD2006-00015) are gratefully acknowledge. L.C.-D. acknowledges the predoctoral fellowship from the Consejería de Educación, Cultura y Deportes del Gobierno Autónomo de Canarias (Beca para Tesis modalidad B2), O. F. acknowledges the FPU Ph.D. fellowship, and F.S.D. acknowledges a postdoctoral fellowship ("Especialización en Organismos Internacionales") from the Spanish Ministerio de Educación y Ciencia.

IC7006765

(33) (a) Burger, K. S.; Chaudhuri, P.; Weighardt, K. *J. Chem. Soc., Dalton Trans.* **1996**, 247. (b) Tamura, H.; Ogawa, K.; Mori, W.; Kishita, M. *Inorg. Chim. Acta* **1981**, *54*, L87. (c) Christou, G.; Perlepes, S. P.; Folting, K.; Huffman, J.; Webb R. J.; Hendrickson, D. N. *J. Chem. Soc., Chem. Commun.* **1990**, 746. (d) Tokii, T.; Nagamatsu, M.; Hamada, H.; Nakashima, M. *Chem. Lett.* **1992**, 1091. (e) Meenakumari, S.; Tiwari, S. K.; Chakravarty, A. R. *J. Chem. Soc., Dalton Trans.* **1993**, 2175. (f) Gutierrez, L.; Alzuet, G.; Real, J. A.; Cano, J.; Borrás, J.; Castiñeiras, A. *Inorg. Chem.* **2000**, *39*, 3608. (g) Gutierrez, L.; Alzuet, G.; Real, J. A.; Cano, J.; Borras, J.; Castiñeiras, A. *Eur. J. Inorg. Chem.* **2002**, *8*, 2094.